Sol−Gel Replication of Microoptical Elements and Arrays

Y. Haruvy,*,† I. Gilath,† M. Maniewicz,‡ and N. Eisenberg‡

SOREQ NRC, Yavne 81800, Israel, and JCT, Jerusalem 91160, Israel

Received April 17, 1997. Revised Manuscript Received September 8, 1997[⊗]

Facile replication of microoptical elements and arrays was performed in sol−gel matrixes prepared by the fast sol−gel method. These sol−gel resins, made from mixtures of alkylalkoxysilane monomers, undergo hydrolysis and polymerization within 10−20 min and curing within a few days. Single-step reproducible fabrication of large crack-free elements of 1 cm thickness and up to 10 cm in diameter was demonstrated. High accuracy of replication was facilitated by maintaining a very small shrinkage of only a few percent during the curing stage. This was attained by removing most of the volatile products from the sol, without gelling, prior to casting it onto the template. Accurate replication depends on adequate control of two key parameters: the replica-template adhesion-separation timing, by manipulating the template surface via oxidative etching, and the drying-cross-linking relative pace, by accurately tailoring the silanes mixture, the water-to-silane ratio, and their hydrolysis and polymerization.

Introduction

Optical microelements and arrays ought to be produced from materials and by processes that ensure high dimensional accuracy, high optical quality, and adequate index of refraction and at a very competitive price compared to other technologies. Glass of various types is the natural candidate material for such applications, whereas the sol−gel synthetic route is very appealing costwise and technologywise.

The sol−gel reaction is a synthetic route by which metal−alkoxide monomers, silane−alkoxides in particular, are converted to ceramic/glassy materials by a sequence of hydrolysis and condensation reactions.[1] The hydrolysis stage (eq 1) involves reaction with water, i.e. catalyzed by an acid or a base, and formation of alcohol. The condensation stage (eq 2) involves formation of M−O−M bonds and results in siloxane macromolecules and small condensates of water or alcohol.

$$\mathrm{Si(OR)_4} \xrightarrow{\mathrm{H_2O}} \mathrm{Si(OR)_3OH} \xrightarrow{\mathrm{H_2O}} \mathrm{Si(OR)_2(OH)_2} \xrightarrow{\mathrm{H_2O}} \mathrm{SiOR(OH)_3} \xrightarrow{\mathrm{H_2O}} \mathrm{Si(OH)_4} \quad (1)$$

$$\equiv\mathrm{SiOH} + \mathrm{HOSi}\equiv \xrightarrow{-\mathrm{H_2O}} \equiv\mathrm{Si{-}O{-}Si}\equiv; \quad \equiv\mathrm{SiOH} + \mathrm{ROSi}\equiv \xrightarrow{-\mathrm{ROH}} \equiv\mathrm{Si{-}O{-}Si}\equiv \quad (2)$$

Sol−gel methods have been extensively investigated for the fabrication of optical elements, both passive and active.[2] Sol−gel-derived siloxane matrixes are of special interest for the encagement of chromophore molecules that facilitate the fabrication of optically active elements, nonlinear optical (NLO) ones in particular,[3−4] in which chromophore−molecules of high NLO activity are discretely encaged in the matrix.

The preparation of glass monoliths or films by the sol−gel method is typically a cautious and prolonged process.[1] This is necessitated by extensive cracking of siloxane matrixes upon rapid drying. The drying also involves great shrinkage which complicates the preparation of optical elements from sol−gel-derived glass.

The new fast sol−gel method recently introduced[5−8] enables facile preparation of siloxane-based glassy materials in which polymerization is completed within minutes and curing within a few hours. The fast sol−gel synthesis employs methyl-substituted alkoxysilane monomers and yields crack-free films as long as the *average* number of alkyl groups per silane equals, or is greater than, 1:[5]

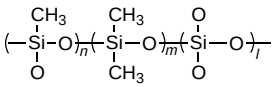

$$(n + 2m)/(n + m + l) \geq 1 \quad (3)$$

Encagement of relatively high concentrations of discrete guest molecules in these new glassy matrixes, aiming at various aspects of nonlinear optics,[5,7,9] has also been demonstrated. Recently, a comprehensive

† SOREQ NRC, Yavne 81800, Israel.

‡ JCT, Jerusalem 91160, Israel.

[⊗] Abstract published in *Advance ACS Abstracts,* November 1, 1997.

(1) Brinker, C. J., Scherer, G. W. *Sol−Gel Science: The Physics and Chemistry of Sol-Gel Processing*; Academic Press: San Diego, CA, 1990.

(2) *Sol-gel optics. II*, Proc. SPIE 1758, Mackenzie, J. D., Ed.; 1992.

(3) Chemla, D. S. Zyss, J., Eds. *Nonlinear Optical Properties of Organic Molecules and Crystals*; Academic Press: New York, 1987.

(4) Zyss, J., Ed. *Molecular Nonlinear Optics;* Academic Press: New York, 1994.

(5) Haruvy, Y.; Webber, S. E. Supported Sol−Gel thin film glasses embodying laser dyes. I. A new fast method for the preparation of optically clear polysiloxane thin-film glasses. *Chem. Mater. 3*, **1991**, 501−507.

(6) Haruvy, Y.; Webber, S. E. Fast Sol−Gel Preparation of Glasses, U.S. Pat. 5,272,240, 1993.

(7) Haruvy, Y.; Heller, A.; Webber, S. E. *Sol-Gel Preparation of Optically Clear Supported Thin-Film Glasses Embodying Laser Dyes−Novel Fast Method*, ACS Symp. Series 499 (*Supramolecular Architecture: Synthetic Control in Thin Films and Solids*), Bein, T., Ed.; American Chemical Society: Washington, DC, 1992; Chapter 28.

(8) Y. Haruvy and S. E. Webber, The fast sol−gel synthetic route to supported glass films: synthetic features, scope, applications and mechanistic studies. *Mater. Res. Symp. Proc.* **1992**, *271*, 297−302.

S0897-4756(97)00229-9 CCC: $14.00

study of the chemical and physical processes involved in curing of this glass and the consequent encaging of guest molecules has been carried out.[10,11]

Cast molding of optical components reduces the time otherwise required for cutting and polishing and speeds up serial production. Molding is further attractive for production of microlenses and microlenses arrays, where fabrication technology is even more complex and expensive.[12] Another advantage of this method is the possibility to incorporate optically active components in the solution of reagents and in the glass thereafter, thus attaining a molecular dispersion of the dopants. Further, the relatively low temperature required for the sol−gel method facilitates use of a wide variety of temperature-sensitive dopants such as organic dyes.

The pioneering sol−gel industrial fabrication of microoptical elements and arrays was established in 1985.[13] However, even in their mature process a substantial shrinkage is still involved in the curing stage, which may either impede the fabrication of very complex elements and arrays or greatly increase the already high cost of production. The optical quality of films obtained by the fast sol−gel method and the facile route of preparation makes this method technologically and economically attractive for microlenses and microoptical arrays.

Microoptical elements and arrays are densely patterned and may contain sharp curvatures. Replication of such elements and arrays imposes strict physical and chemical requirements on both the templates and the sol−gel prepared replicas. These requirements need to be addressed by the chemistry of the materials involved, either the bulk or the surface chemistry.

The chemical properties of the mold are of crucial importance for the replication. Durability to swelling is mandatory for dimensional accuracy. Great surface polarity is required for good adhesion of the resin to the mold throughout the glass curing. However, this surface polarity must be limited to allow for separation of the cured glass elements from the mold. The problems related to these aspects of the replication are presented, and the solutions attained by chemical manipulation of the mold materials are discussed.

The chemical nature of the viscous sol−gel prepared resin is of crucial importance for the crack-free drying of the glass. The chemical constitution must allow gelling-free removal of the volatile reaction products from the sol prior to replication, which is necessary to minimize the shrinkage. The sol structure must enable slow cross-linking concurrently with substantial relaxation, which is crucial for crack-free drying of the glass. The problems related to these aspects of the replication are presented and the solutions attained by chemical manipulation of the mold and the sol−gel processes of polymerization and curing are discussed.

Experimental Section

Monomers and Reagents. Methyltrimethoxysilane (MTMS), tetramethyl orthosilicate (TMOS) (Aldrich, CP), and dimethyldimethoxytsilane (Hulls, CP) were used as alkoxysilane monomers and employed without further purification; 10^{-2} M HCl (CP) was employed as catalyst for the sol−gel reaction, 6 M NaOH (CP) was employed for etching the support materials and patterned templates, and deionized water and acetone (CP) were used for cleaning the support materials and templates.

Supports. Glass slides (1 mm thick), Kapton films (75 μm thick), and AsSe chalcogenide films (25 μm thick on 1 mm glass slides[14]) were used as flat support materials for the sol−gel casting. Patterned supports were made of polycarbonate and PMMA (Fresnel Lenses), cured photoresist, cured polyimide resin, and gold-sputtered metal slabs. For improved adhesion, slight surface etching of the supports was carried out by dipping in 6 M NaOH, 24 h for glass, 5 min for plastic. This etching was followed by rinsing in deionized water and drying. Surface oxidative etching of plastic supports was carried out employing a RF oxygen plasma generator (Harrick Plasma Cleaner) at various operation conditions.

Sol−Gel Procedures. The experimental setup is described in detail elsewhere.[5] A typical procedure runs as follows. First, a water bath is placed on a heating/stirring plate and stabilized at the selected temperatures, between 80 ± 2 and 98 ± 2 °C (boiling). Into a 8 mL vial equipped with a screw cap and a small magnetic bar are quickly weighed 1 g of MTMS (7.35 mM) and 0.198 g of 10^{-2} M HCl (11 mM). The water-to-silane molar ratio (MR) in this recipe is 1.5. Molar ratios of 1.4−1.8 were also employed.

The vial is sealed tightly and placed in the water bath to allow stirring while heating to the reaction temperature. When the violent initial reaction relaxes, the screw cap is cautiously removed, and the vial is placed again in the water bath to allow evaporation of the produced methanol. The reaction progress, manifested by vigorous boiling and loss of weight, is monitored gravimetrically. Casting and spin coating are carried out at the highest viscosity that still allows casting, typically at a weight loss of 0.5−0.575 g per 1 g of MTMS in the recipe.

For the preparation of large elements, the procedure was extended to 40 g of silane and the corresponding, finely tailored amount of HCl (about 8 g). Removal of the volatile products was accelerated by vacuum out-distillation of the alcohol, gradually applied after a weight loss of about 21 g. Weight loss maintained prior to casting ranged between 22 and 24 g.

Casting and Replication. Casting of microoptical elements (MOEs) is carried out on supports that are either flat or patterned. Patterning depth ranges from 5 to 200 μm. Three procedures of casting were employed. Spin coating is employed for the preparation of supported sol−gel glass films. The supports for these are either flat or finely patterned (negative imprinting) with MOEs of small depth (e.g. 5−25 μm).

Casting is employed for thicker MOEs (e.g. 50−250 μm), on the appropriate supports or templates, to produce either supported or self-supporting glass elements. Special molds have been prepared for the preparation of thick elements, where the bottom was made from etched support material and the boundaries made of Parafilm. These molds enable the casting of weighted quantities of resin onto well-defined areas of the support. Imprinting onto cast or spin-coated sol−gel, when partly cured, is employed for composite elements.

Particulate contamination in the produced microoptical elements was eliminated by filtration of all the reagents (0.45 μm filter). Filtration of the sol−gel viscous resin prior to casting was also practiced to eliminate particulate material that may be produced during the sol−gel process.

Curing. Typical curing procedures consist of 24 h at ambient temperature and humidity, followed by 24 h at 65 °C. Vacuum-distilled resins are cured directly at 65 °C. For

(9) Lebeau, B.; Maquet, J.; Sanches, C.; Toussaere, E.; Hierle, R.; Zyss, J. Relaxation Behavior of NLO Chromophores Grafted in Hybrid Sol−Gel Matrixes, *J. Mater. Chem.* **1994**, *4*, 1855.
(10) Chambers, R. C., Jones, W. E , Jr.; Haruvy, Y.; Webber, S. E.; Fox, M. A. Influence of Steric Effects on the Kinetics of Ethyltrimethoxysilane Hydrolysis in a Fast Sol−Gel System. *Chem. Mater.* **1993**, *5*, 1481.
(11) Hibben, Q.; Lu, E.; Haruvy, Y. Webber, S. E. Fast Sol−Gel Thin Films: Thermal and Corona-Field Accelerated Curing. *Chem. Mater.* **1994**, *6*, 761.
(12) *Microlenses;* Wu, H. D., Barnes, F. S., Eds.; IEEE Press: 1991.
(13) Geltech, Corporate Profile and Data Package, 1996.
(14) Lyubin, V.; Klebanov, M.; Bar, I.; Eisenberg, N. P.; Manievich, M. Novel Effects in Inorganic $As_{50}Se_{50}$ Photoresists and their Application in MicroOptics. *J. Vacuum Sci. Technol. B* **1997**, *15*, 4.

Table 1. Separation of PMSO Thin Films Cast onto Kapton Etched by O-plasma

kapton etching parameters	adhesion of the PMSO resin[a]	separation of thin glass films (<50 μm)	remarks
pristine	good	spontaneous - complete	separation observed after partial curing[b]
100 torr of O_2; 0.5 min of etching	very good	spontaneous - partial separation	separation with cracking
100 torr of O_2; 3.0 min of etching	very good	spontaneous - none; mechanical - difficult	good separation of very thick films (>500 μm)

[a] All resins were cast at maximum viscosity (just before gelling), after removal of at least 0.5 g of methanol per 1 g of MTMS. [b] All samples were cured 24 h at rt followed by 24 h at 65 °C.

extended MOE stability, slow heating (10 °C/h) to 250 °C is sometimes employed. For quick testing of thin elements (< 1 mm), the cast sol−gel is cured 1 h at 100 °C.

Stability Analysis. MOE samples were tested, following various procedures of casting and curing, to determine their durability to solvents and reagents. Exposure methods include wetting, soaking for 24 h at room temperature, and soaking for 24 h at 65 °C. Solvents tested include acetone, THF, and ethanol. Reagents tested were 0.1 M HCl and 1 M NaOH.

Temperature stability was tested up to 250 °C. Laser durability was tested at power densities, pulse durations, and frequencies relevant to desired applications.

Chemical Analysis. Chemical analysis was carried out by FTIR (Nicolet, Model DX-5) and XPS (X-ray Photoelectron Spectroscopy; Kartos Analytical, Model HS-AKIS). Surface analyses were carried out at the air-facing surface of the sol−gel, its support-facing surface (following separation), and at the surface of the support following replication and separation of the sol−gel derived glass.

Morphology. SEM (JEOL, Model 6300, and Phillips, Model 525/535), AFM (Digital Instruments, Model Nanoscope-II), and ZYGO 3D imaging surface structure analyzer (an imaging-processing optical nanoscope) were employed for morphological analysis of the MOE surfaces. Surface morphology was studied in flat and patterned MOE at the air-facing and support-facing surfaces and the surface of the support materials.

Results, Observations, and Discussion

Supports and Sol−Gel Adhesion and Separation. Photolithography is the most common technique for the preparation of patterned molds, and photoresists are typically employed for this purpose. However, molds made of common photoresists tend to swell following casting of sol−gel-derived resins, even after the alcohol is removed from the resin by extensive out-distillation. This can be attributed to the inherent swelling power of oligomeric siloxane resins. Sol−gel-derived resins were also found capable of swelling, or even solvating, other polymers unless the latter are highly cross-linked or crystalline. This has directed us to choose highly cured polyimide for the preparation of supports and patterned molds.

Studying the various aspects of adherence and separation of the sol−gel resins to polymeric support materials was the foremost effort. For the preparation of free-standing elements, we need a support surface that provides sufficient adhesion to the sol−gel while it undergoes curing, while allowing it to separate when cured. These two requirements are in accord since in the course of curing hydroxy and methoxy groups at the gel surface undergo condensation. The resulting enrichment of the surface with methyl groups substantially decreases the gel−mold adherence forces. Hence, the support surface must have a high, yet controlled, density of polar groups that enables attachment of the resin but not permanent chemical bonding.

To manipulate the timing of adhesion/separation sequence we may choose to modify the adhesion properties of either the support or the resin. However, any change in the siloxane resin may adversely affect its crack-free stress-free curing into an optical element. It is much preferred to tailor the resin to meet the needs of crack-free curing of the *sol−gel bulk*, and tailor the support *surface* to meet the needs of adhesion to the *sol−gel surface*.

The adherence onto the supports can be substantially increased by a few minutes etching in 6 N NaOH or oxygen plasma. Pristine Kapton provided sufficient adhesion for the preparation of films ca. 25 μm thick. Early separation of the glass and its distortion in films thicker than 500 μm necessitated surface treatment of the Kapton support. Chemical etching in NaOH is very effective but difficult to regulate. Oxygen plasma treatment is a well-controllable method for oxidative etching[16] and, hence, adequate for delicate manipulation of the support's surface polarity.

The adhesion/separation characteristics of sol−gel-derived resins cast onto oxygen plasma etched Kapton are summarized in Table 1. The surface density of polar groups in pristine Kapton is insufficient to hold the gel throughout the curing. Kapton subjected to 0.5 min plasma treatment adheres to thin films (<50 μm) sufficiently strong to eliminate premature detachment. Thicker MOEs (>500 μm) necessitate 3 min of plasma treatment to hold them onto the Kapton to the end of curing, and this was found to be a general trend: on a given support, the thicker the cast element, the earlier it starts to separate.

Surface Chemical Analysis. Characterization of the modified surfaces of the supports is necessary to reproducibly control the timing of adhesion and separation. SEM and AFM were found suitable for studying the etching-produced roughness, whereas FTIR and XPS have been employed for chemical characterization, oxygen content in particular. The latter is most adequate to indicate the surface polarity of the support and, hence, the timing of sol−gel resins adhesion and separation.

Selected FTIR data are summarized in Table 2 and the XPS data in Table 3. All samples were cured for 24 h at room temperature (rt) and 24 h at 65 °C. XPS was carried out on cured films following their separation from the polyimide supports. Selected FTIR and XPS spectra are shown in Figures1 and 2, respectively.

The FTIR absorption data (cf. Table 2) was recorded for sol−gel films attached to the Kapton support and processed by subtracting the spectrum of the Kapton. The $CH_3-Si\equiv$ peak at 2974 cm^{-1} was employed as an internal reference to compensate for thickness varia-

(15) Haruvy, Y.; Heller, A.; Webber, S. E. *Supported Sol-Gel Thin-Film Glasses Embodying Laser Dyes. II. Three Layered Assemblies of Polymethylsiloxane Thin Films Prepared by the Fast Sol−Gel Technique.* In *Proc. SPIE Symp.* 1590, *Submolecular Chemistry and Physics*; Bray, P., Kreidl, N. J., Eds.; p 59, SPIE, 1991.

(16) Vered, R. The Effects of Atomic Oxygen and Ion-Beams on Polymeric Materials. Ph.D. Thesis, Soreq NRC and The Hebrew University, 1996.

Table 2. FTIR of Sol−Gel Thin Films

a. MTMS

sol−gel		relative peak height[a,b]			
composition of reactants HCl/MTMS (MR)	procedure of preparation *T*, °C; Δ*W* (w/w)[c]	$CH_3OSi\equiv$/ $CH_3Si\equiv$	$HOSi\equiv$/ $CH_3Si\equiv$	remarks	sample code
MTMS (1 g); HCl MR = 1.40	*T* = 95 ± 1 °C MeOH evap: 0.500 g	0.33	1.12	crack-free, undetached	001
		0.30	1.04	crack-free, undetached	002
MTMS (1 g); HCl MR = 1.40	*T* = 95 ± 1 °C MeOH evap: 0.550 g	0.29	1.08	crack-free, partly detached	006
MTMS (1 g); HCl MR = 1.43	*T* = 95 ± 1 °C MeOH evap: 0.500 g	0.15	1.59	crack-free, undetached	007
		0.22	1.38	crack-free, partly detached	008
MTMS (1 g); HCl MR = 1.43	*T* = 95 ± 1 °C MeOH evap: 0.550 g	0.33	1.09	crack-free, partly detached	011
		0.24	1.27	crack-free, partly detached	012
MTMS (1 g); HCl MR = 1.50	*T* = 95 ± 1 °C MeOH evap: 0.500 g	0.12	1.66	crack-free, partly detached	016
MTMS (1 g); HCl MR = 1.50	*T* = 95 ± 1 °C MeOH evap: 0.525 g	0.15	1.54	crack-free, partly detached	018
MTMS (1 g); HCl MR = 1.80	*T* = 95 ± 1 °C MeOH evap: 0.525 g	0.10	0.97	crack-free, undetached	019
		0.05	1.35	crack-free, fully detached	020

sol−gel		relative peak height[a,b]			
composition of reactants HCl/(DMDMS + TMOS)	procedure of preparation *T*, °C; Δ*W* (w/w)[c]	CH_3-O-Si≡/ CH_3-Si≡	H-O-Si≡/ CH_3-Si≡	remarks	sample code
MIX (1 g); HCl MR = 1.40	*T* = 95 ± 1 °C MeOH evap: 0.575 g	0.40	0.96	cracked, partly detached	024
		0.58	1.08	cracked, partly detached	025
MIX (1 g); HCl MR = 1.40	*T* = 95 ± 1 °C MeOH evap: 0.575 g[d]	0.44	1.12	crack-free, partly detached	026
MIX (1 g); HCl MR = 1.43	*T* = 95 ± 1 °C MeOH evap: 0.575 g	0.50	1.00	crack-free, partly detached	027
MIX (1 g); HCl MR = 1.80	*T* = 95 ± 1 °C MeOH evap: 0.525 g	0.30	0.91	cracked, undetached	039
		0.36	0.99	cracked, undetached	040
MIX (1 g); HCl MR = 1.80	*T* = 95 ± 1 °C MeOH evap: 0.575 g	0.29	0.88	cracked, undetached	037

[a] Film average. [b] $CH_3Si\equiv$ at 2974 cm^{-1} (reference); $CH_3OSi\equiv$ at 2844 cm^{-1}; $HOSi\equiv$ at ~3370 cm^{-1}. [c] Spin-cast: 4 min at 700 rpm. [d] Spin-cast: 4 min at 1000 rpm.

Table 3. XPS of Sol−Gel Thin Films

		concentration of atomic species (%)[a]									
		sol−gel: air-facing surface			sol−gel: Kapton-facing surface			Kapton:[b] sol−gel facing surface			
sol−gel composition of reactants	sol−gel procedure of preparation	C 1s	O 1s	Si 1s	C 1s	O 1s	Si 1s	C 1s	O 1s	Si 1s	sample code
Kapton support								70.7	21.5	1.8	blank[c]
MTMS (1 g): HCl MR = 1.40	*T* = 95 ± 1 °C MeOH evap: 0.5 g	42.2	37.8	20.0	32.4	43.5	24.1				001
MTMS (1 g): HCl MR = 1.43	*T* = 95 ± 1 °C MeOH evap: 0.5 g	31.6	44.6	23.8	30.4	45.4	24.2				007
MTMS (1 g): HCl MR = 1.80	*T* = 95 ± 1 °C MeOH evap: 0.525 g	28.2	47.5	24.3	30.3	45.1	24.6	70.4	22.0	2.8	019

[a] H% is not recorded. [b] N% is not specified. [c] Samples 1−19: spin-cast onto untreated Kapton, 4 min at 700 rpm.

tions.[11] The $CH_3-O-Si\equiv$ peak at 2844 cm^{-1} and the $H-O-Si\equiv$ peak at about 3370 cm^{-1} were used for characterizing the degree of curing in the sol−gel films. It can be expected that the more cross-linked the sol−gel is, the lower the normalized peak intensities, [$CH_3-O-Si\equiv/CH_3-Si\equiv$] and [$H-O-Si\equiv/CH_3-Si\equiv$], become. Theoretically, in a fully cured film these peaks should disappear following their reaction to form $\equiv Si-O-Si\equiv$ groups.

The FTIR data (Table 2a) show that hydrolysis of the methoxy groups requires a water-to-silane molar ratio (MR) of at least 1.8 to near completion, above the stoichiometric ratio of MR = 1.5. This is reasonable since 1.5 moles of water (per mole of silane) hydrolyze only 1.5 out of the 3 moles of alkoxy groups. The remaining groups are consumed during the condensation process, the completion of which is impeded by steric hindrance. The relatively low MR is employed deliberately, to attain slow cross-linking necessary for casting, patterning, and crack-free drying. A slightly substoichiometric MR was found advantageous for the preparation and patterning of large and thick elements (ca. 5 cm in diameter and 1 cm thick).

The degree of methanol evaporation only slightly affects the FTIR, particularly at the higher MR. This finding reflects the small relative changes in the ratios of moles of methanol removed per mole of silane: 2.125, 2.23, 2.34, and 2.44 mol/mol at 500, 525, 550, and 575 mg evaporated, respectively. These ratios are not too far apart to be differently manifested in the residual methoxy groups. They do, however, strongly manifest in the degree of polymerization and resin viscosity thereafter.

The 1:1 mixture of DMDMS and TMOS (Table 2b) results in higher concentrations of residual methoxy groups. This explains well why films spin cast from these resins adhere properly to etched supports but poorly onto untreated supports. The residual concentration of the $Me-O-Si\equiv$ groups and the corresponding detachment from the supports decrease upon increase of the MR but not to the same extent as in the MTMS derived resins (Table 2a).

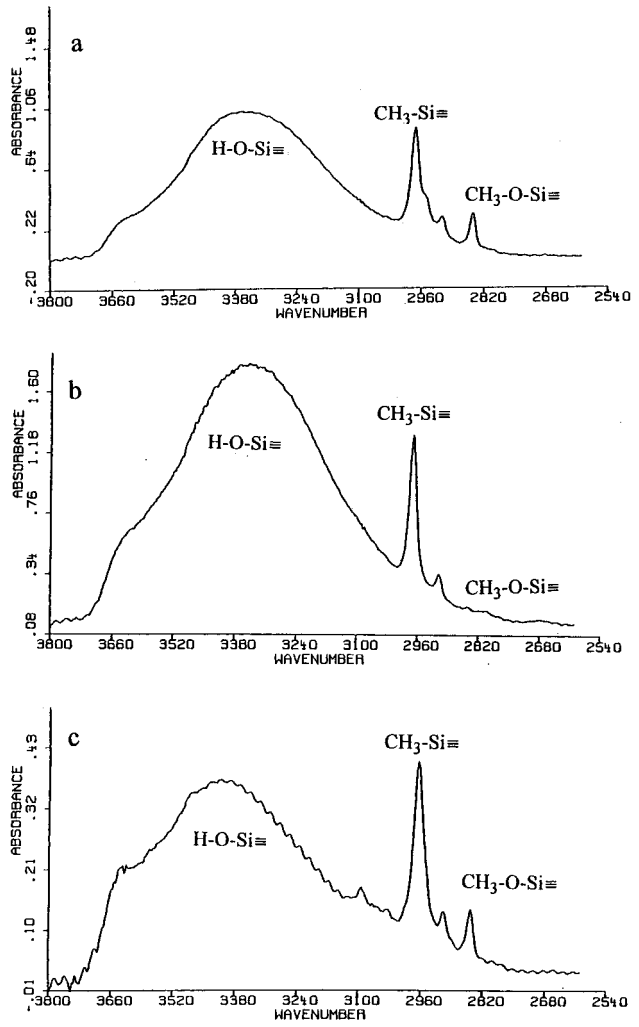

Figure 1. Selected FTIR spectra of the sol−gel films: (a) MTMS, MR = 1.40, MeOH evap. 0.500 g/g MTMS; (b) MTMS, MR = 1.80, MeOH evap. 0.525 g/g MTMSc; (c) TMOS/DMDMS (1:1 m/m), MR = 1.80, MeOH evap. 0.525 g/g MTMS.

The relatively lower concentrations of the HO−Si≡ groups in these resins, even at high MR (cf. Table 2a with Table 2b) is somewhat puzzling. On the average, the MTMS and the 1:1 molar mixture of DMDMS and TMOS have a similar distribution of functional groups. Hence, the difference in the residual groups has to be attributed to different interplay of the hydrolysis and the condensation processes. The most prominent difference is observed at MR = 1.8. The MTMS resin exhibits very low concentration of the residual methoxy, which may result from a rapid hydrolysis of these groups or their condensation with hydroxy groups. The high residual concentration of the hydroxy groups suggests that the high MR induces faster hydrolysis, but the condensation remains rather slow. From similar argumentations, the characteristic FTIR spectrum of the DMDMS/TMOS resins at high MR manifests relatively slower hydrolysis and faster condensation processes as compared to those of the MTMS resins. The faster condensation may be attributed to smaller steric hindrance in the mixed-monomer resins, due to the presence of the dimethoxy-silane groups. These interesting aspects of the condensation are the subject of an ongoing morphological research.

The XPS data in Table 3 show the effect of adjacent material on the sol−gel derived surface composition. In samples 1 and 7 the air-facing surface is richer in carbon, i.e., methyl and methoxy groups, compared to the Kapton-facing surface. Upon casting, both surfaces had identical distribution of methyl, methoxy, and hydroxy groups. During the curing, one side of the sol−gel faces the relatively polar Kapton support, whereas the other side faces the nonpolar air. As already reported,[15] the surface of the sol−gel rearranges its groups to match the polarity of the adjacent surface. Hence, the decrease in concentration of methyl and methoxy groups in samples 1 and 7 at the Kapton-facing surface, accompanied with increased concentration of oxygen, i.e., hydroxy groups, probably manifests the Kapton-induced rearrangement of the sol−gel-derived surface.

In light of this rationale, the data of sample 19 seem puzzling. While its Kapton side is quite similar to that of sample 7, its air side exhibits a much lower concentration of carbon and much higher concentrations of oxygen and silicone. The reasons for this characteristic are most probably both the higher MR and the relative "dryness" of sample 19. The high MR (1.8) in this sample allowed a higher pace of hydrolysis and polymerization, and hence a faster rise in viscosity. The higher degree of methanol out-distillation from this sample further increased its viscosity. It is most likely that its air-side surface became dry and glacial already during the spin casting and could no longer rearrange. The Kapton-side surface in this sample, however, retained sufficient methanol to rearrange.

The XPS data in Table 4 relates to the four types of support materials considered for replication or fabrication of multilayer composite microoptical elements. The surface oxygen content in all four is relatively high, in accord with their strong adherence to sol−gel-derived resins. It is noteworthy that the surface oxygen content of the chalcogenide is lower than the stoichiometric (>50% molar). Nevertheless, its observed adherence to sol−gel-derived resins is very high (cf. Patterning and Replication), manifesting the high polarity of the metal−oxide groups on the surface.

Surface Morphology Analysis. The surface morphology of the sol−gel-produced films and patterned microoptical elements was studied in a wide variety of scales, from the macroscopic and the microscopic scale (SEM) to the nanoscale (AFM and ZYGO optical nanoscope).

In the macroscopic scale we monitored the flatness of the produced element. The support-facing side is indicative of the comparative pace between drying/shrinking and detachment from the support. The air-facing side is indicative of the comparative pace between drying/shrinking and the cross-linking. These observations are important for fine-tuning of the sol−gel recipe, polymerization, and drying.

In spin-cast elements (<100 μm) both surfaces are flat and smooth. In cast elements thicker than 0.5 mm, the support-facing surface is smooth but the air-facing surface sometimes contains wavelets. These elements are characterized by a meniscus due to unmatched shrinkage at the two surfaces during the curing stage, as schematically depicted in Figure 3.

Spin casting of thick elements is impractical, since it results in excessive cracking. This probably manifests a cumulative effect of spinning-induced stresses and inhomogeneous drying-induced stresses. Flatness of cast elements is attained when their thickness exceeded

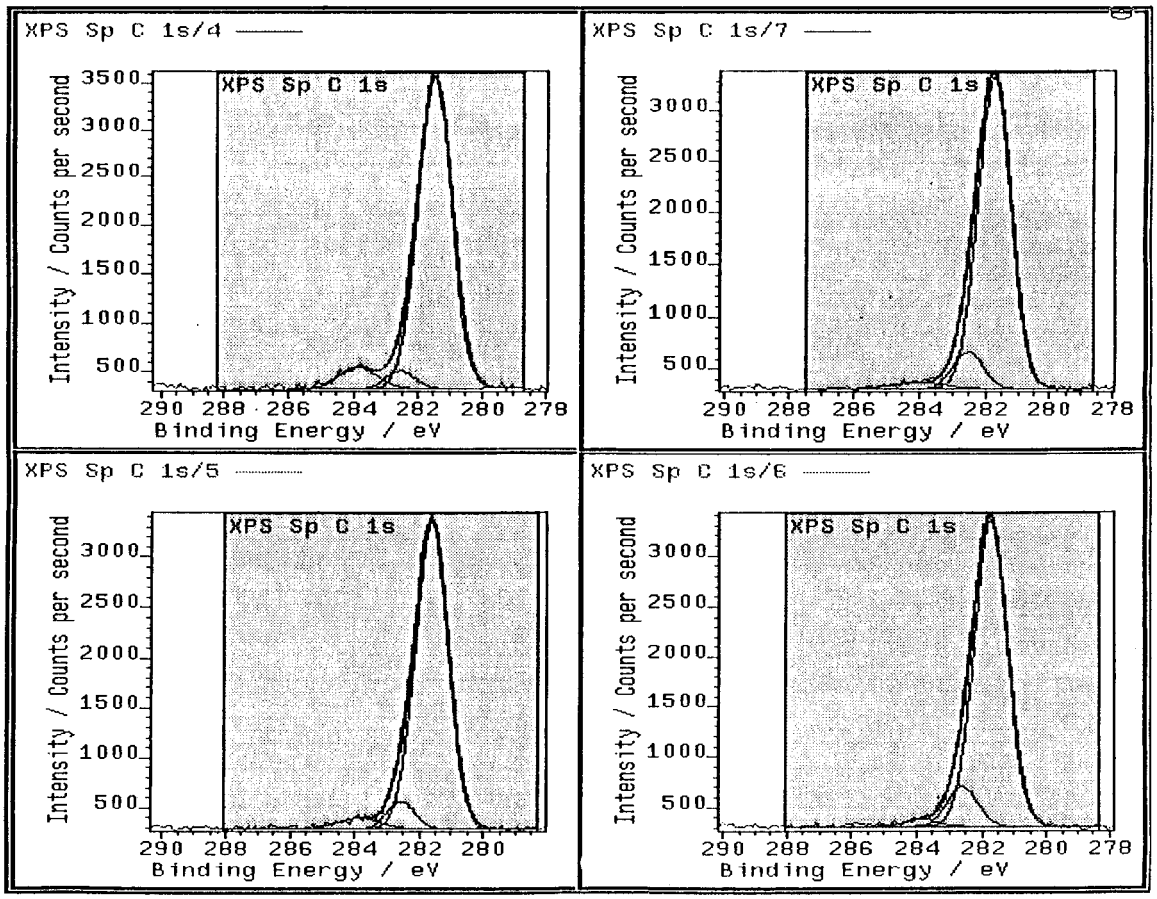

Figure 2. Selected XPS spectra of MTMS derived sol−gel films: (upper) air-facing surface; (lower) Kapton-facing surface. (Left): MR = 1.43, MeOH evap. −0.500 g/g MTMS. Right: MR = 1.80, MeOH evap. −0.525 g/g MTMS.

Table 4. XPS of Support Films

	concentration of atomic species (%)[a]							
support type	C 1s	O 1s	N 1s	Si 1s	Na 1s	Se 1s	As 1s	remarks
Kapton - commercial film (yellow)	70.7	21.5	6.0	1.8				
Kapton - resin cured at 250 °C (yellow)	65.8	27.8	2.4	3.4	0.6			surface probably oxidized
Photoresist - positive, cured (blue)	65.7	28.1	2.9	3.3				
Chalcogenide - solid (red) [group of Prof. V. Lyubin]		20.8				49.6	29.6	

[a] H% is not recorded.

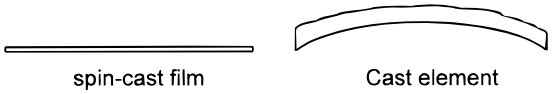

Figure 3. Macroscopic observed differences between spin-cast (thin) and cast (thick) elements. The thickness and waviness are not to scale.

5 mm, since at this thickness the glass is no longer capable of bending. The air-surface wavelets are eliminated by slowing down the drying, e.g. by carrying it in closed containers, or by patterning the elements on both sides.

In the microscopic scale (SEM), we monitored small irregularities in flatness, formation of defects, microcracks, or particulate contamination. SEM photographs of all crack-free samples prepared by spin casting show highly smooth surfaces at both sides, as can be expected from a liquid-originated matrix. Small particulate material, ca. 0.5 μm in diameter, was sometimes found embedded in the samples. This is a known feature of the fast sol−gel process[5] and is believed to result from early formation of excessively cross-linked moieties in the resin and their microphase separation thereafter.[11] Filtration of the viscous resin prior to the casting completely eliminates this problem. Finally, microscopic morphological analysis of patterned and replicated sol−gel-derived microoptical elements was carried out as well and is discussed in a later subsection.

In the nanoscale, AFM photographs of several sol−gel spin cast unpatterned films are shown in Figure 4. The extreme smoothness of the sol−gel surface is in accord with its liquid origin. The tiny flaws observed in the air-facing surface may result from inhomogeneous drying and surface shrinkage thereafter, or microphase separation.[11] In the support-facing surface, the degree of smoothness replicates the smoothness (or patterns) of the mold.

Patterning and Replication. Replication experiments necessitate support materials that enable post-curing crack-free separation of the sol−gel-derived glass from the support. The high oxygen content of both glass and chalcogenide supports, and the consequently observed strong adherence to sol−gel cast on them, made these supports suitable only for the fabrication of multilayer composite microoptical elements. For rep-

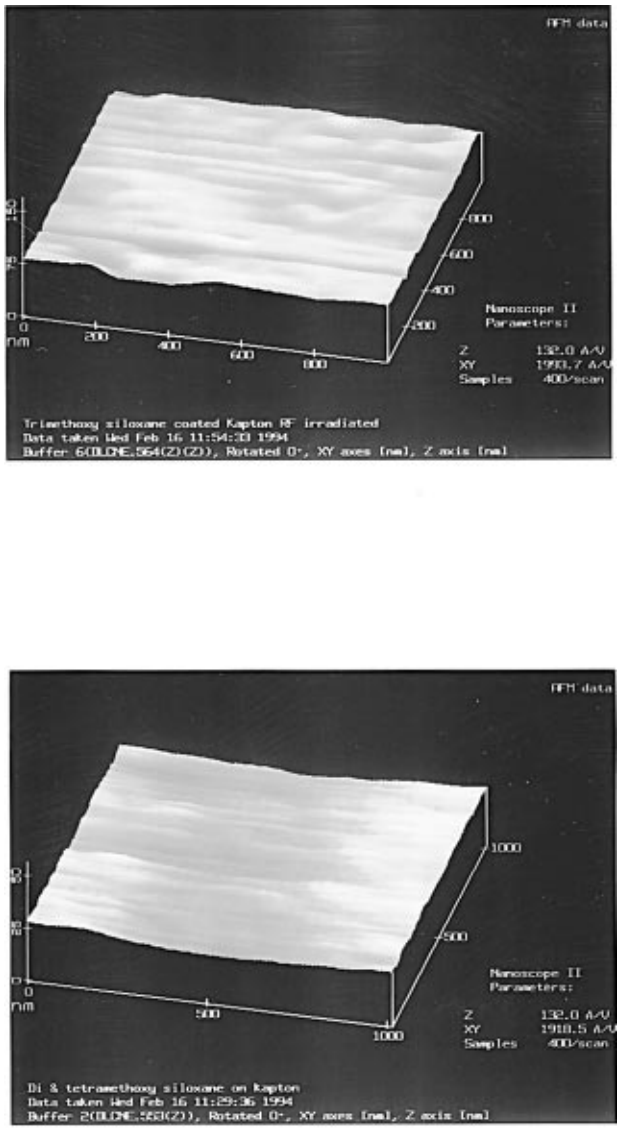

Figure 4. AFM photographs of several sol−gel spin-cast films. Top: MTMS derived film. Bottom: TMOS/DMDMS (1:1 m/m) derived film.

lication, polymeric supports were found superior to glass and chalcogenide supports.

Replication experiments were first carried out on segments of a Fresnel Lens. The viscous sol−gel-derived resins were spin-coated (25−50 μm dry thickness) on the patterned segments or cast without spinning (100−2000 μm dry thickness). All samples have been cured 24 h at rt followed by 24 h at 65 °C. The resulting replicas have been compared with their templates by SEM, as shown in Figures 5a−d and 6. The prominent observation is the "better" surface quality of the replica, as compared to that of the template. This has to be attributed to inaccessibility of small scratches, pinholes, and tiny defects to the viscous resin.

This is seemingly an advantage that helps to "mend" minor imperfections in the template, thus yielding replicas of better surface quality. This is further demonstrated in the replication of a gold surface with some rough shallow grooves (50−200 μm wide) shown in Figures 7a,b. The grooves are precisely replicated excluding most of the imperfections in the template.

The Replication Factor. When replicating μ-optical elements (MOEs) and arrays in sol−gel-derived resins, the inaccessibility of sharp or very small "true" patterns to the highly viscous resin becomes an obstacle. Also, small replicated patterns may undergo excessive shrinkage in the course of drying due to the increasing surface tension of the siloxane resin. Inaccurate replication of tiny patterns may defect the optical functioning of the replicated MOEs. Thus, we have to investigate the correlation between the dimensions of the small patterns and the accuracy of their replication in the viscous sol−gel resin.

The primary question is how small can the radius of curvature in a pattern be and still become accurately replicated? We define a replication factor for each radius of curvature as the ratio between radii of a replicated optical curvature (r_2) and its template (r_1). This factor is an obstructing factor that needs to be experimentally studied and then synthetically manipulated to attain the desired micropatterns. The expected relationship between r_2/r_1 vs r_1 is schematically depicted in Figure 8.

Replication should preferably be carried out in the flat region of the curve. However, if our microoptical arrays comprise small curvatures, some of them may be in the steep region of this curve. Then, we may need to shift the r_2/r_1 curve in our process to include all the curvatures in the flat region. This can be attained by manipulation of the sol−gel synthetic route: the lower the resin viscosity obtained, the more the r_2/r_1 curve shifts to the right. However, any change in the sol−gel may tamper its crack-free drying or even its attachment to the support throughout the process of curing.

Two ways are suitable for shifting the r_2/r_1 curve to the right. One way is by increasing the adhesion of sol−gel resin to the template. This can be attained by increased etching of the template surface, e.g. by O_2 plasma oxidative etching. Manipulation of the template may, however, hamper the separation of the glass μ-optical array from the mold. The second way may be by reverse engineering of the templates, as well as by reverse engineering of the optical elements themselves. Right now, from Figures 5−7, it seems that the flat part of the r_2/r_1 curve ranges well below 100 μm.

The Shrinkage Factor. The overall volume shrinkage in elements prepared by the fast sol−gel process is smaller than 10%. This shrinkage is a crucial factor controlling the accuracy of replication. It manifests foremost an interplay between two processes simultaneously occurring in the glass: drying and cross-linking. Accurate replication necessitates minimizing the shrinkage. This is achieved by maintaining minimal weight loss and slow cross-linking that allows relaxation and, thus, crack-free curing. An additional element in the shrinkage factor is anisotropy resulting from the adhesion to the mold. Thus, no planar shrinkage can take place during the curing stage, only perpendicular. This anisotropic drying is advantageous for the accuracy of replication. However, it may induce stresses in the course of cross-linking that may cause some shrinkage of the glass after its separation from the mold and replication inaccuracy thereafter. The obstacle of residual stresses can be eliminated to a large extent by fine-tuning of the water-to-silane near-stoichiometric molar ratio in the mixture of reagents.

Minimizing the weight loss is a primary means for reduction of the shrinkage. Practically, the further we evaporate the methanol formed in the reaction, the smaller the weight loss and shrinkage during the

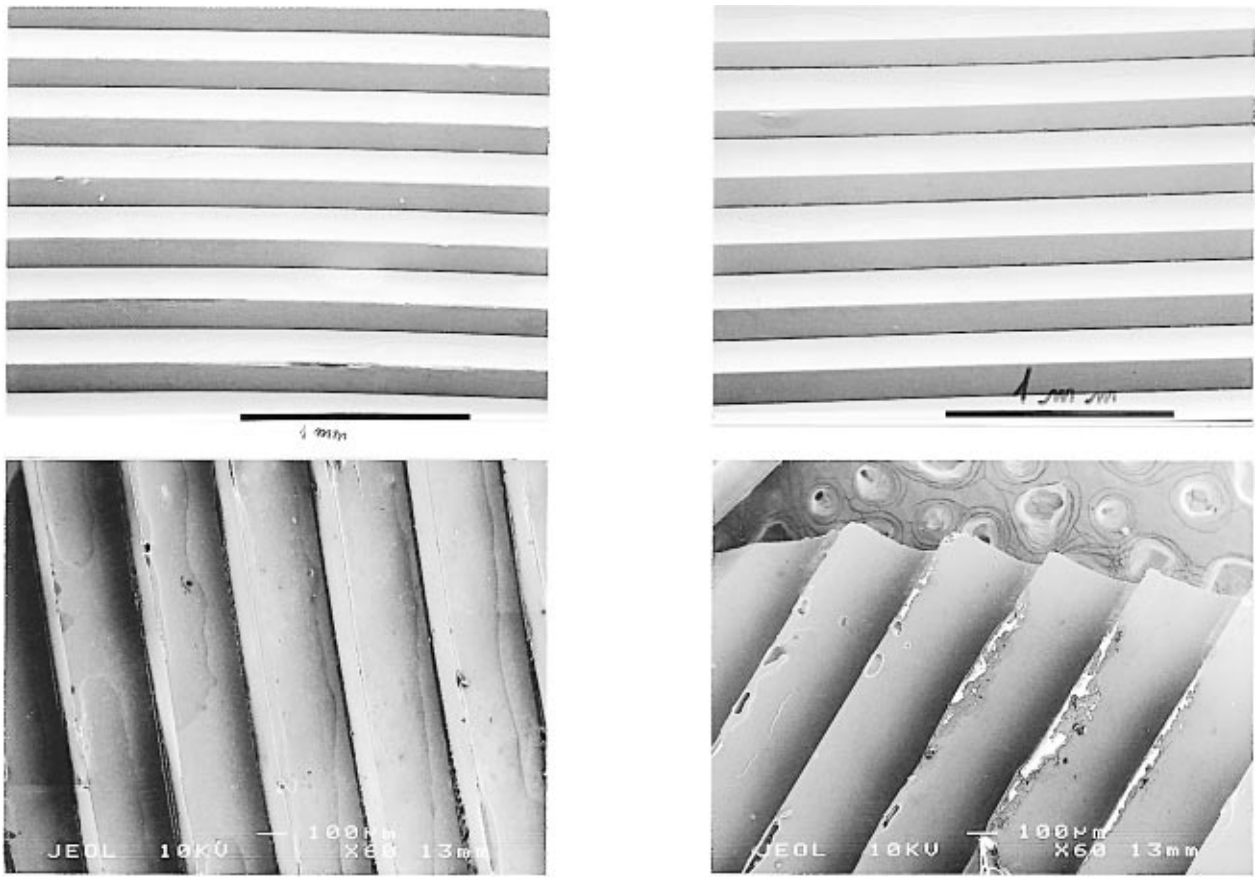

Figure 5. SEM photographs of replicated Fresnel lenses. Top: top view. Bottom: side view. Left: PMMA templates. Right: sol−gel replicas.

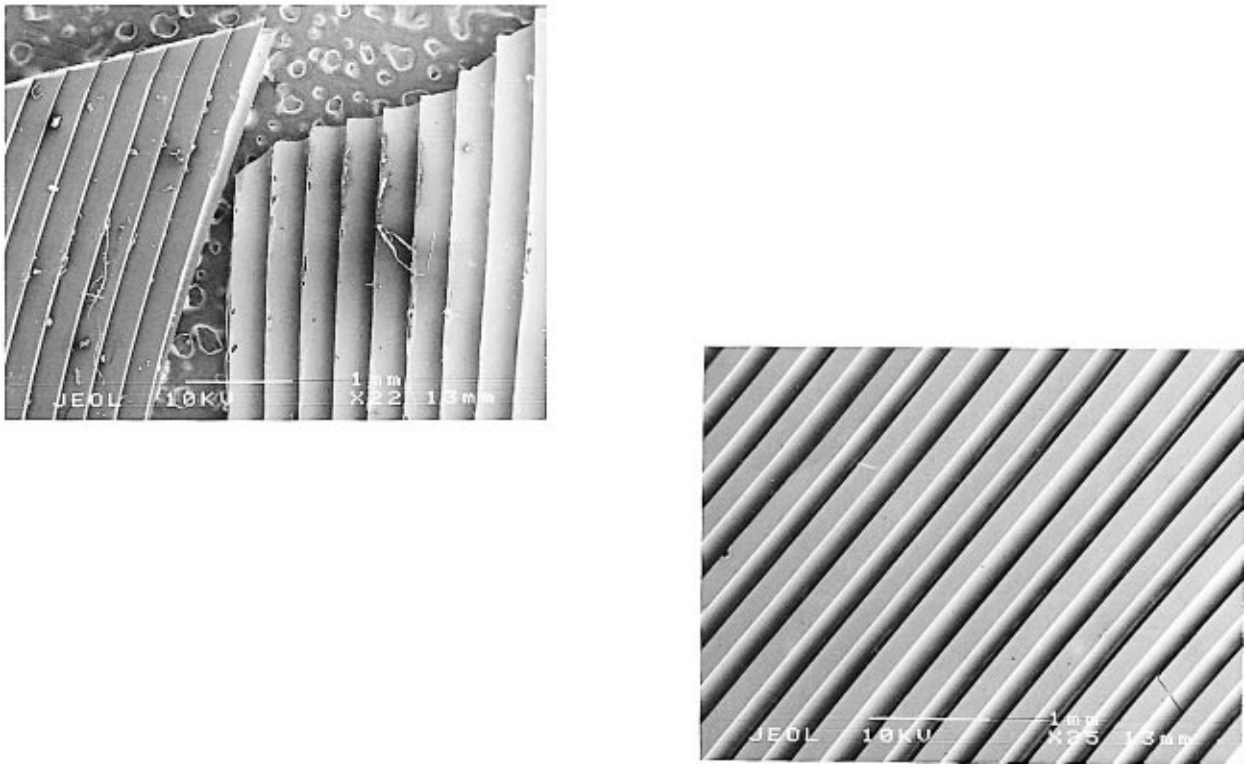

Figure 6. SEM photographs of replicated microoptical arrays. Top: Fresnel lens, template (left) and sol−gel replica (right). Bottom: replica of specialty Lockheed diffractive lens.

drying. This, however, increases the viscosity of the cast sol and shifts the r_2/r_1 curve (cf. Figure 8) to the left. Therefore, accurate replication requires a well-balanced combination of fine tailoring of the template surface polarity and the sol−gel resin viscosity upon casting. The tailoring required for the template surface depends also on the actual patterning. Templates for replicating densely patterned μ-optical arrays have relatively higher effective surface areas, e.g., about 2.4 times higher than the nominal for an array of spherical elements. The

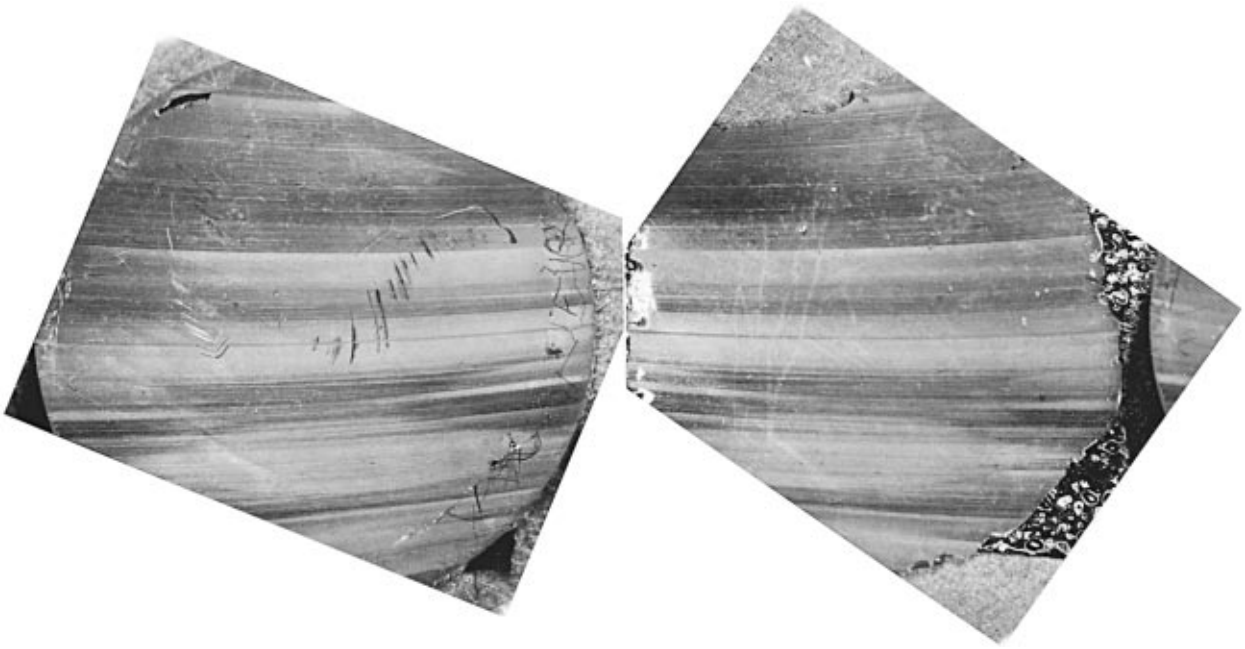

Figure 7. SEM photographs of sol−gel replication of gold-coated machined brass rod. Left: template. Right: sol−gel replica.

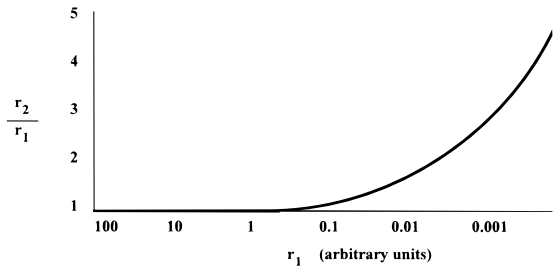

Figure 8. Schematic of an expected relationship between r_2/r_1 and r_1.

higher the surface area, the stronger the resin−template adhesion, and the lesser the degree of oxidative-etching needed. Therefore, for μ-optical arrays of exceptional patterning density we may need a specific tailoring of the resin viscosity and template surface polarity.

In Figure 9, the mold and replica of standard USAF three bar test chart (Ealing Electro Optics no. 26-6809) are shown. The negative mold was photolithographically imprinted onto a glass-supported polyimide film and cured at 250 °C. The cast sol−gel-derived resin (MTMS, MR = 1.43) was cured (24 h at 25 °C; 24 h at 65 °C) and the replica was separated from the templates. The sol−gel replication appears very precise, with a shrinkage of about 8% (within the error limits) as compared to the polyimide template. The smallest feature in the array thus replicated was a 8×2 μm^2 cylindrical lens.

The data from these replication experiments is insufficient for studying the replication factors typical of our resins, since the shrinkages of all the elements in this array are very close. The poor stereoscopic resolution obtained by SEM also impedes correct assessment of the replication factors. Far more precise data were obtained by the ZYGO 3D imaging surface structure analyzer, which is an image-processing optical nanoscope. For this purpose, an array of negative microcylindrical elements was photolithographically prepared from polyimide resin. The diameters of the microcylindrical elements range from 5 to 50 μm. A sol−gel-derived resin from which the alcohol was vacuum out-distilled (to <50% w/w of the original weight) was employed for this replication. The replica thus prepared was 12 mm thick and 25×25 mm^2 in size.

The template and sol−gel replica are shown in Figure 10. The cylindrical lenses in the reproduced array appear smooth and accurately replicated from the template. The polyimide template after the replication looks identical with that before replication, implicating their possibility of its multiple use. The differences in diameter between the template and the replica were found negligible in the entire range (5−50 μm), manifesting that the replication factor curve at this range is practically one. Since this is the most useful range of patterning for microoptical arrays, the road is apparently open to approach the development of a process for their industrial fabrication. Since in the course of years, smaller and smaller microelements are desired, the ongoing research aims at determining the replication factor for smaller diameters, in the range of 0.5−50 μm.

Development of the Fast Sol−Gel Route To Enable Thick Elements. The classical sol−gel routes to silica-made films[1] were practically limited to a thickness of 1 μm. The early fast sol−gel routes[5−8] have extended this capability to a thickness of about 100 μm. This thickness already enabled replication of microoptical elements, but their mechanical strength was insufficient for convenient handling.

The new goal of thick elements mandated extrarelaxation properties to eliminate cracking. This demand has led to extreme change of the sol−gel recipe, lowering the water-to-silane molar ratio from 1.65 to 1.80 to 1.43−1.50, and from a reaction at 80−90 to 98−100 °C. These changes resulted in a 2-fold manipulation of the reaction. Shifting the recipe to a substoichiometric MR slows down the cross-linking, thus extending the time for internal relaxation processes. The increase in temperature probably results in an enhanced formation of dimers and, hence, the formation of ladder segments. The resulting lower fraction of hydrolyzed monomeric species is believed to result in a slower formation of side groups capable of cross-linking, as depicted in Figures 11a,b. This may also further extend the time span for

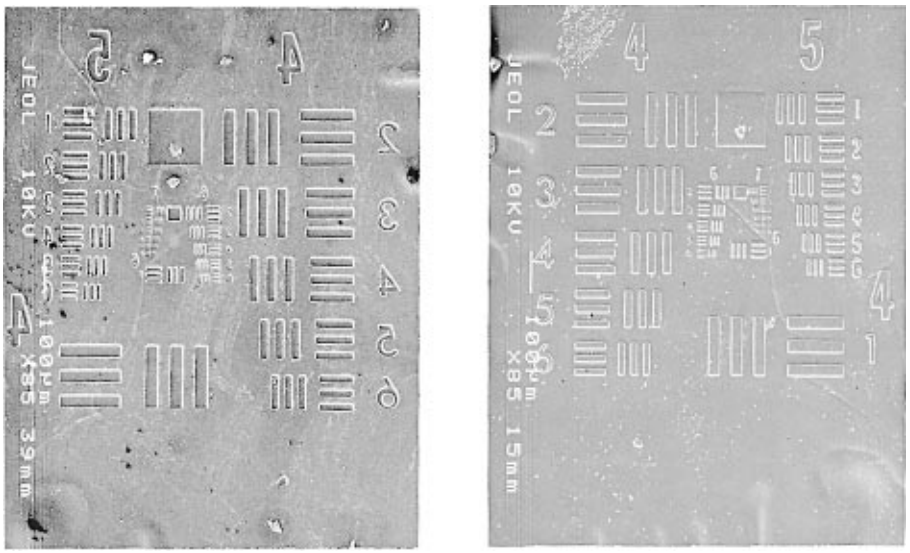

Figure 9. SEM photographs of US Air Force Calibration Template made of polyimide (left) and its sol−gel replica (right). All samples are sputtered with gold.

processes of internal relaxation. Vacuum out-distillation of the alcohol further assists in reducing the cast volume and, hence, the shrinkage upon curing.

There is, however, a penalty for these changes. The higher content of ladder segments accompanied by the formation of fewer side groups results in a low density of active groups at the surface of the glass, resulting in a weaker adhesion to the template and early detachment from the support. To cope with it, the time of O_2 plasma treatment of the support materials must be extended. As a result, a facile single-step replication of microoptical arrays was obtained. Self-supporting sol−gel-derived patterned glasses with thickness of up to 12 mm and diameter of up to 10 cm were thus prepared for various experiments and applications. As can be expected, the larger the elements, the higher the oxidation of the support and the further the vacuum out-distillation of methanol that are needed.

The suggested structure of ladder-like segments in Figure 11 is extrapolated from the structure commonly ascribed to polyphenylsilasequioxane.[16] It is argued, in view of our observations of lasting rubber-like flexibility in the elements produced, that prior to completion of their curing enables, for example, folding or rolling of 0.5 mm thick elements without any cracking. Small percentage of residual SiOR groups in the semicured sol−gel (cf. FTIR data in Table 2) prohibits attributing the flexibility to a single-strand polymer, implying the formation of double-strand Si−O−Si-bridged polymer segments and chains.

The suggested structure is currently being investigated by microwave time−domain dielectric spectroscopy[18] and is strongly supported by findings of transition phenomena typical of polymers rather than ceramics. ^{17}O NMR spectroscopy of the solid sol−gel glass[19] will also be employed to try and excerpt direct evidence about the structure, aiming at determining the percentage of oxygens in four-member ring structures of the ═Si(Me)−O− unit (cf. Figure 11).

Stability of Replicated MOEs. For each type of MOE there was found a set of parameters of the sol−gel process that facilitate crack-free preparation and curing. The thus prepared sol−gel MOEs can withstand single-stage rapid curing temperatures of up to 120 °C. Slow curing at 65 °C for a couple of days endow a temperature stability range of −180 to 200 °C. Slow crack-free heating is possible up to 250 °C (10 °C/h), but it results in cracking upon cooling, unless the cooling is slowed to ∼1 °C/min. These observations are in accord with the extended curing of apparently cured sol−gel glass found at the temperature range of 200−250 °C.[11] The durability of the MTMS derived sol−gel spin-cast glass films to pulsed laser energy was found comparable to that of commonly used optical glass. The durability of thick elements was found, however, to be extremely sensitive to surface smoothness and bulk residual stresses, which are the primary topic of the currently ongoing research on sol−gel-derived microoptical elements and arrays.

Fully cured sol−gel MOEs made of pure MTMS were found to be highly resistant to concentrated acids and nonpolar organic solvents, even after 24 h of soaking at 65 °C. Like most glasses, these sol−gel elements are slowly etched and dissolved in concentrated base (i.e. 6 N NaOH). The sol−gel elements are unaffected by ethanol, but slight swelling takes place following a few hours of immersion in THF and acetone. A slight modification of the silane mixture, employing TMOS and DMDMS, facilitates the preparation of MOEs that are highly resistant to concentrated acids and most organic solvents (24 h, 65 °C). The inherent sensitivity of these sol−gel elements to aqueous NaOH still remains, as the surface-mounted methyl groups have insufficient density to mask the siloxane matrix and block the hydrolysis.

Conclusions

The study of the fundamental aspects of replication of microoptical elements and arrays in sol−gel-derived glass has led to several breakthroughs in this art:

(17) *Silicon Compounds Register and Review*, 5th ed.; Anderson, R., Larson, G. L., Smith, C., Eds.; Hüls: Piscataway, NJ, 1991, p 280.

(18) Feldman, U.; Andrianov, A.; Polygalov, E.; Ermolina, I.; Romanichev, G.; Zuev, Y.; Milgotin, B. Time Domain Dielectric Spectroscopy: An Advanced Measuring System. *Rev. Sci. Instrum.* **1966**, *67*, 3208.

(19) Babonneau, F.; Gualandris, V.; Pauthe, M. *NMR Characterization of the Chemical Homogeneity in Sol-Gel Derived Siloxane-Silica Materials*, ACS Symp. Series 435; Coltrain, B. K., Sanchez, C., Scherer, D. W., Wilkes, G. L., Eds.; American Chemical Society: Washington, DC, 1996; p 119.

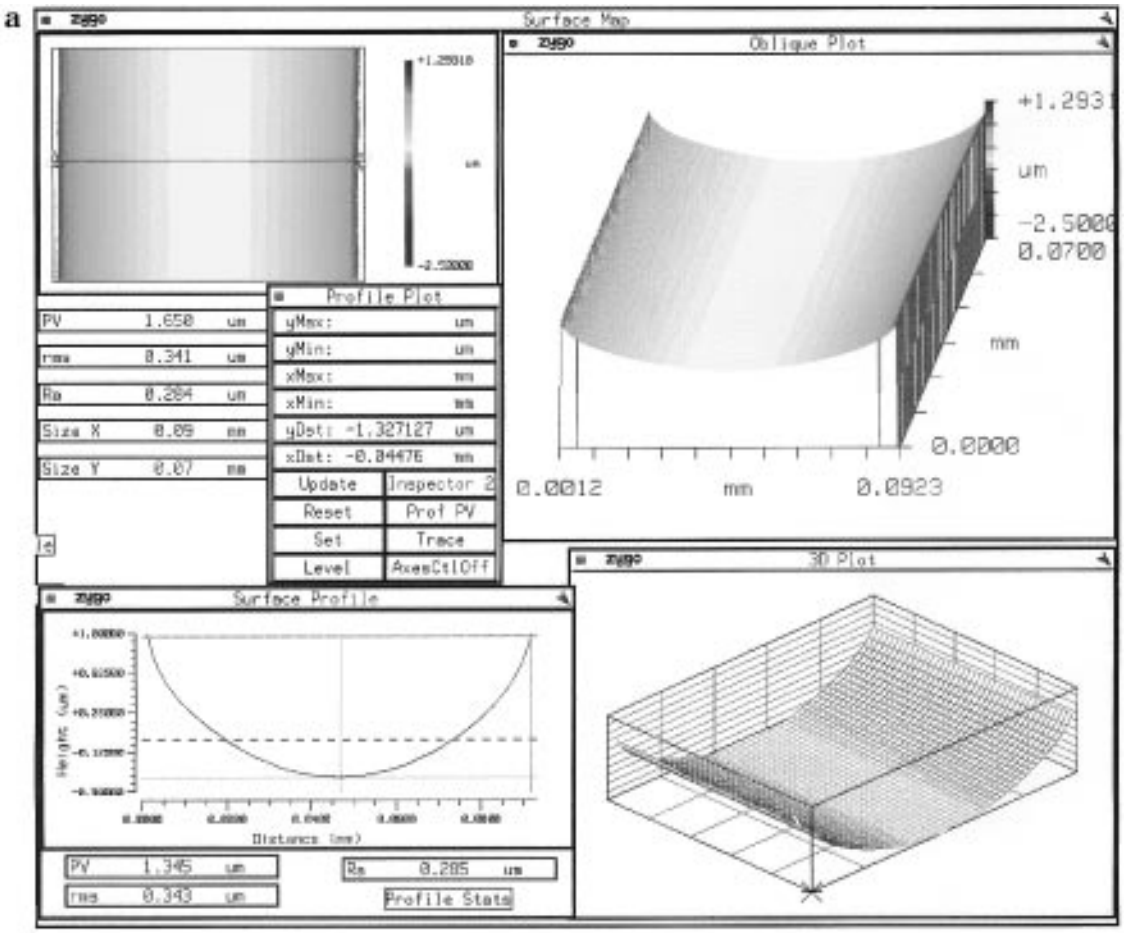
a
Surface Map
Oblique Plot
Profile Plot
3D Plot
Surface Profile
PV 1.658 um
rms 0.341 um
Ra 0.284 um
Size X 0.09 mm
Size Y 0.07 mm
yMax:
yMin:
xMax:
xMin:
yDat: -1.327127 um
xDat: -0.04476 mm
Update
Inspector 2
Reset
Prof PV
Set
Trace
Level
AxesCtlOff
+1.2931
um
-2.5000
0.0700
mm
0.0000
0.0012
mm
0.0923
Height (um)
Distance (mm)
PV 1.345 um
rms 0.343 um
Ra 0.285 um
Profile Stats

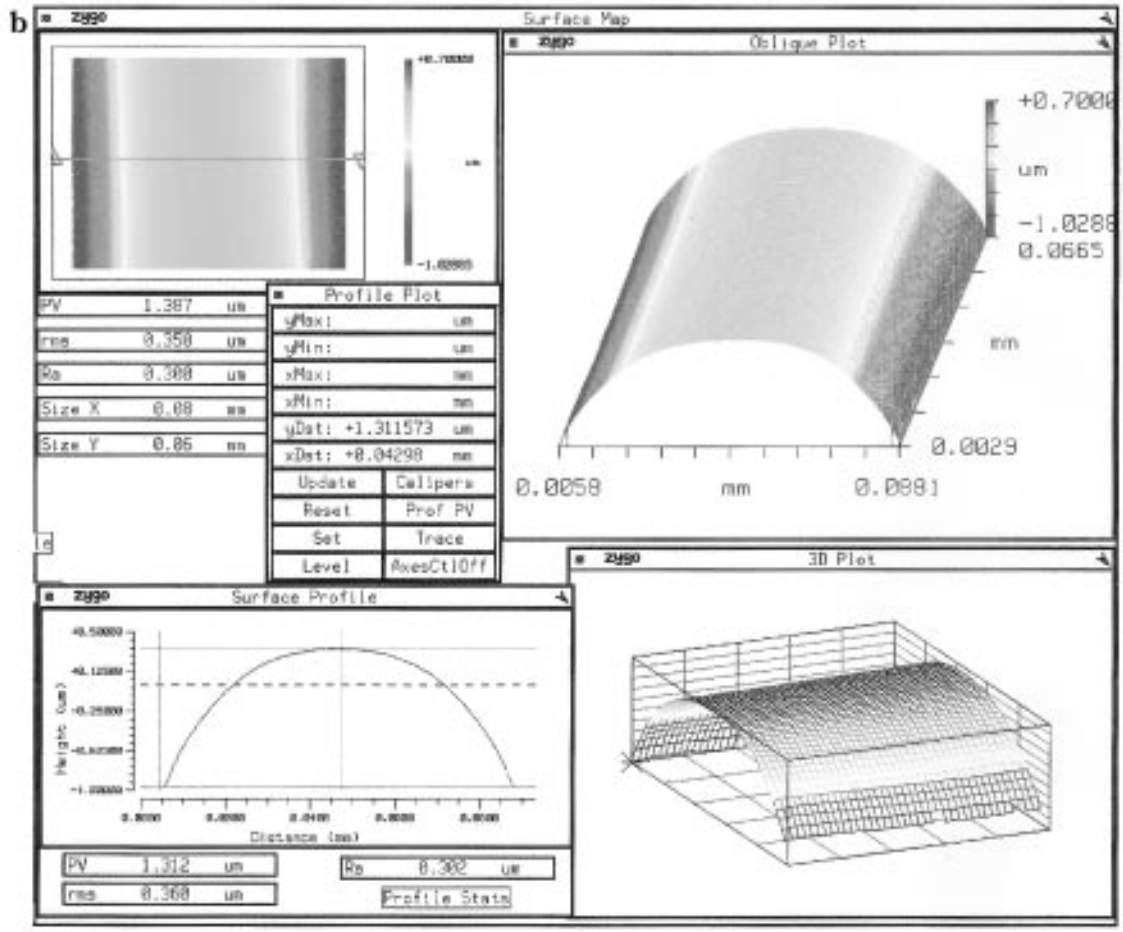
b
Surface Map
Oblique Plot
Profile Plot
3D Plot
Surface Profile
PV 1.387 um
rms 0.350 um
Ra 0.300 um
Size X 0.08 mm
Size Y 0.06 mm
yMax:
yMin:
xMax:
xMin:
yDat: +1.311573 um
xDat: +0.04298 mm
Update
Calipers
Reset
Prof PV
Set
Trace
Level
AxesCtlOff
+0.7000
um
-1.0288
0.0665
mm
0.0029
0.0058
mm
0.0881
Height (um)
Distance (mm)
PV 1.312 um
rms 0.300 um
Ra 0.302 um
Profile Stats

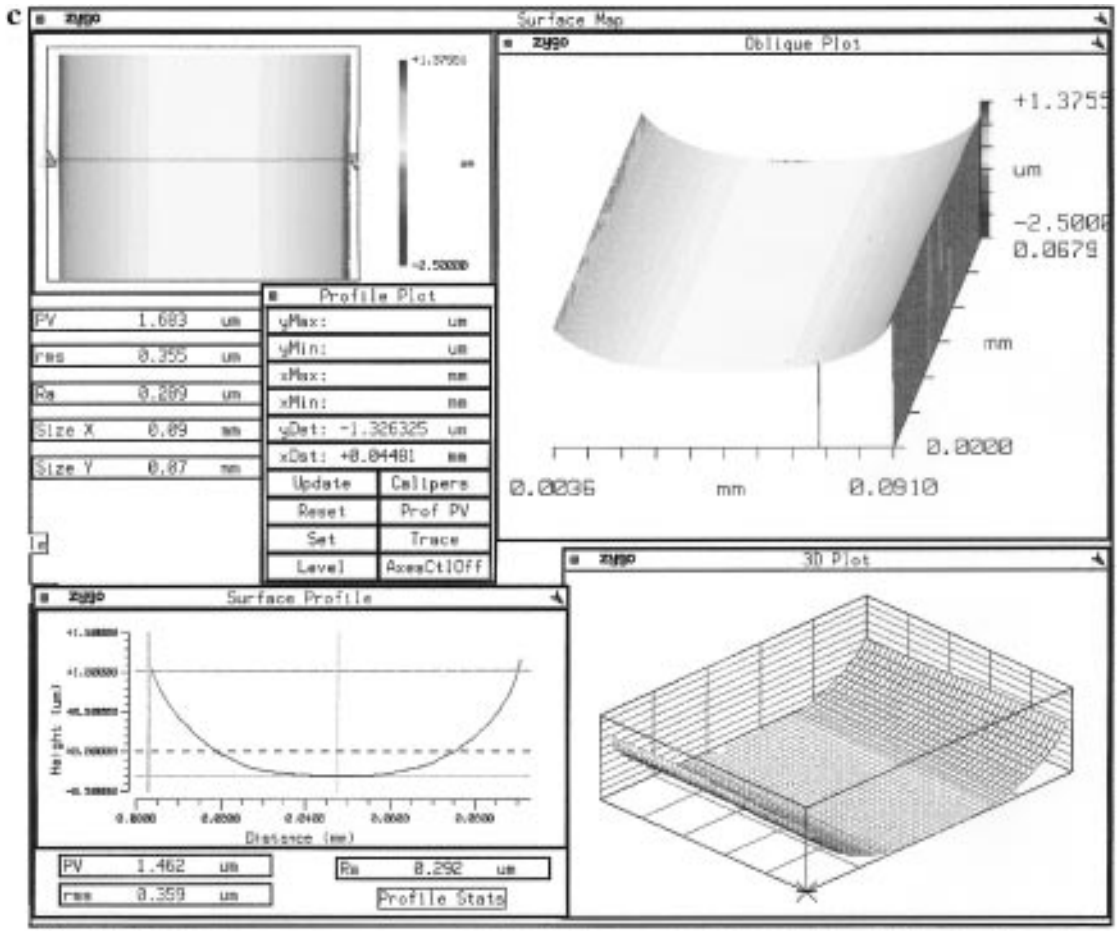

Figure 10. Polyimide negative template and positive sol−gel replica of microcylindrical elements array. The elements diameter range from of 5 to 50 μm: (a) Pristine template; (b) sol−gel derived replica; (c) post-replication template.

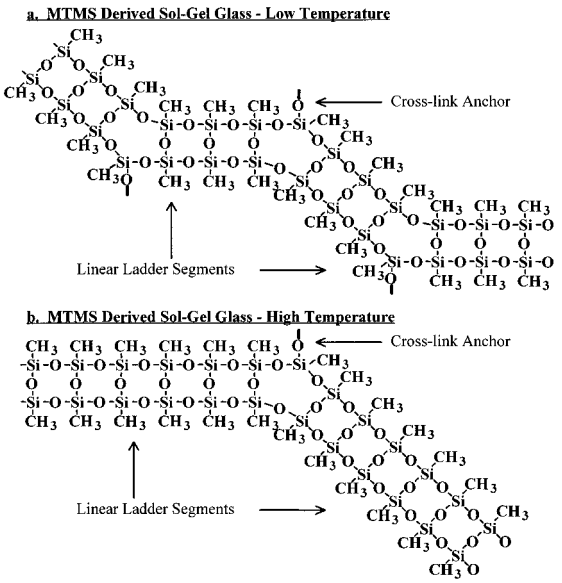

Figure 11. Linear segments and cross-linking anchors in MTMS derived sol−gel glass.

1. Identification of the controlled modification and quantitative analysis of the support surface oxygen content as the primary means for prompt self-timing of the glass-support detachment, that is, chemical tuning of the time, in the course of the process of curing, at which the contraction of the sol−gel matrix overcomes the forces of its adherence to the support.

2. Identification of the need for specifically tailored sol−gel chemical constitution, degree of polymerization, and alcohol out-distillation as the primary means to ensure the mechanical and stability features of the glass.

3. As a result, a facile single-step replication of microoptical arrays was obtained. Self-supporting sol−gel-derived glass patterned elements with thicknesses of up to 12 mm and diameters of up to 10 cm were thus prepared for various experiments and applications.

Acknowledgment. The authors express their gratitude for the financial support of this research by the Ministry of the Science and the Arts, contract no. 8559-1-95.

CM970229M